# PARAMETERS IDENTIFICATION OF BODNER-PARTOM MODEL FOR FLUID IN MR DAMPER

**Paweł SKALSKI[*,***] , Krzysztof WOŹNICA[**] , Jerzy BAJKOWSKI[***]**

[*]Institute PRISME, University of Orleans, France
[**]Institute PRISME, Bourges Higher National School of Engineering, France, 88 Boulevard Lahitolle, 18020 Bourges
[***]Institute MDF, Faculty of Automotive and Construction Machinery, Warsaw University of Technology, Narbutta 84, 02-524 Warszawa

p.skalski@azspw.pl, krzysztof.woznica@ensi-bourges.fr, jba@simr.pw.edu.pl

**Abstract:** This paper presents an approach to describe a dynamic behaviour of magnetorheological damper by the Bodner-Partom constitutive law. The B-P equations usually used for metals are presented for shear stresses to express viscoplastic proprieties of MR fluid. Material parameters for the B-P law for fluid in the LORD RD 1005-3 damper are determined. Experimental results are compared with numerical results.

## 1. INTRODUCTION

Magnetorheological (MR) fluids like electrorheological (ER) fluids are a kind of smart material whose rheological properties may be rapidly varied by application of a magnetic field. This material typically consists of micron-sized ferrous particles dispersed in a fluid. When MR fluid is exposed to a magnetic field, the liquid state may be changed to semi-liquid or extremely to a solid state. When the magnetic field is removed, the state may recover to liquid. The speed of changes of rheological properties are an order of milliseconds. Controlled by computer and modern control methods, magnetorheological fluid can be used in all kinds of dampers (Carlton and Jolly, 2000; Spencer et al., 1996). Dampers with MR fluids may offer an improved control of vibrations in airplanes upon landing, and in cars, mechanical devices, and industrial machinery.

The main aim of this paper is to present a preliminary approach to parameters identification of the B-P law for fluid in the MR damper. The Bodner-Partom equations (Boder et al., 1979) usually used for metals are presented for shear stresses to express the viscoplastic proprieties of MR fluid.

## 2. EXPERIMENTS

Experiments have been conducted at a vertical stand for MR dampers with the forced kinematical movement, at Warsaw University of Technology. Installed sensors allowed to measure and record values of damping forces, and displacement of the piston rod during movement. The scheme of the stand was described in Bajkowski (2005) and is neglected here.

The research schedule included series of tests with one value of current $I$=1A with the different speed of forced kinematic movements $n_1$=100rpm, $n_2$=200rpm, $n_3$=400rpm. All experiments were carried out with the Rheonetic RD 1005-3 damper from Lord Corporation (Jimenez and Alvarez-Icaza, 2005).

## 3. MODEL AND PARAMETERS IDENTIFICATION

Results of the test for three different shear rates are the basis for the determination of parameters. During tests, values of displacements $x$, force $F$, and time $t$ were recorded. Afterwards, the shear stress $\tau$, the shear strain strain $\gamma$, the inelastic shear strain $\gamma^I$ and the inelastic shear rate $\dot{\gamma}^I$ can be calculated respectively:

$$\tau = \frac{F}{A}, \gamma = \frac{\Delta x}{h}, \gamma^I = \gamma - \frac{\tau}{G}, \tag{1}$$

$$\dot{\gamma}^I = \frac{d\gamma^I}{dt} = \dot{\gamma} - \frac{1}{G}\frac{d\tau}{d\gamma}\dot{\gamma}, \tag{2}$$

where $A$ and $h$ stand for the working interface area and the gap size, and $G$ is the shear modulus. Fig. 1 presents the shear strain-shear stress relation for three different shear rates. These relations served for the identification of the Bodner-Partom model.

In this case of neglecting the recovery effects, the constitutive formulation of Bodner-Partom can be expressed in the following form (Woźnica et al., 2001):

$$\dot{\gamma}^I = 2D_0 \exp\left[-\frac{1}{2}\left(\frac{R+D}{\sqrt{3}\tau}\right)^{2n}\frac{n+1}{n}\right]\operatorname{sgn}(\tau), \tag{3}$$

$$R = R_1\left[1 - \exp\left(-m_1 W^I\right)\right] + R_0 \exp\left(-m_1 W^I\right),$$

$$D = D_1\left[1 - \exp\left(-m_2 W^I\right)\right], \tag{4}$$

where $R$ represents the isotropic hardening, $D$ is the function associated to the kinematic hardening. The parameter $D_0$, that designates the maximal value of the shear rate, can be chosen arbitrarily. In almost static problems, one admits $D_0=10^4 s^{-1}$ (Chan et al., 1998). $D_1$, $R_0$, $R_1$, $m_1$, $m_2$, $n$ are the parameters to be identified and $\dot{W}^I = \tau\dot{\gamma}^I$ is the inelastic work rate. The relation (3) can be written as a functional relationship between the shear stress, the inelastic shear rate and the hardening variables,

$$\frac{\tau}{R+D} = f\left(\dot{\gamma}^I\right). \tag{5}$$

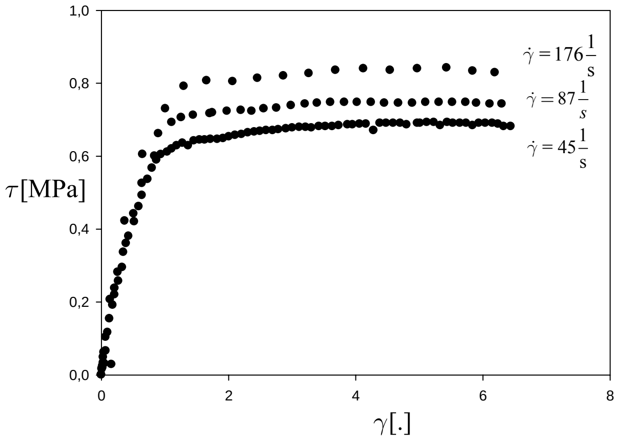


**Fig. 1.** Shear stress as a shear strain function-experimental data for three different shear rates

The identification of $n$ and $R_0$ parameters can be carried out from Eqs. (5), expressed for small values of inelastic shear strain (e.g., $\gamma^I$=0,2%), for several different shear rates. When the material enters in the plastic domain, one can consider that the isotropic hardening is equal to its initial value $R=R_0$, and the kinematic hardening is negligible. The initial yield stress function of the shear rates is written according to (3):

$$\tau_{02} = \frac{R_0}{\left[\frac{2n}{n+1}\ln\left(\frac{2D_0}{\sqrt{3}\dot{\gamma}^I}\right)\right]^{\frac{1}{2n}}}. \tag{6}$$

Having several values of $\tau_{02}$ for different shear rates, the diagram $\tau_{02}\left(\dot{\gamma}^I\right)$ can be drawn (Fig. 2) and by the least squares method non linear regression, $n$ and $R_0$ values can be determined.

Subsequently, the inelastic shear strain $\gamma^I$, Eq. (1), is calculated to construct the curve $\tau(\gamma^I)$ for every test, and this curve can be approximated by the multi parameter exponential function (Fig. 3):

$$\tau = a\left(\gamma^I\right)^b \exp\left(c\gamma^I\right) + d, \tag{7}$$

where coefficients $a$, $b$, $c$ and $d$ can be determined by the Marquardt-Levenberg regression. It permits of the derivative:

$$\frac{d\tau}{d\gamma^I} = a\left(\frac{b}{\gamma^I} + c\right)\left(\gamma^I\right)^d \exp\left(c\gamma^I\right), \tag{8}$$

which is used to draw the function of the work hardening rate $\psi$, Fig. 5:

$$\psi = \frac{d\tau}{dW^I} = \frac{d\tau}{d\gamma^I}\cdot\frac{1}{\tau}; \quad dW^I = \tau\cdot d\gamma^I. \tag{9}$$

Taking into account formulas (3-6), the hardening work rate function (9) can be written in the following form:

$$\psi = \frac{\tau_0}{R_0}\left[m_1\left(R_1 - R\right) + m_2(D_1 - D)\right]. \tag{10}$$

Supposing for the small inelastic shear strains $R=R_0$ (Border et al., 1979), and using (3) and (6), formula (10) becomes:

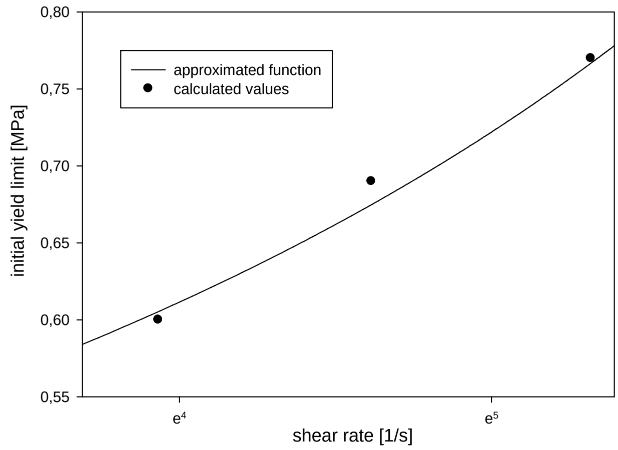


**Fig. 2.** Conventional yield limit for the B-P model as a function of strain rate

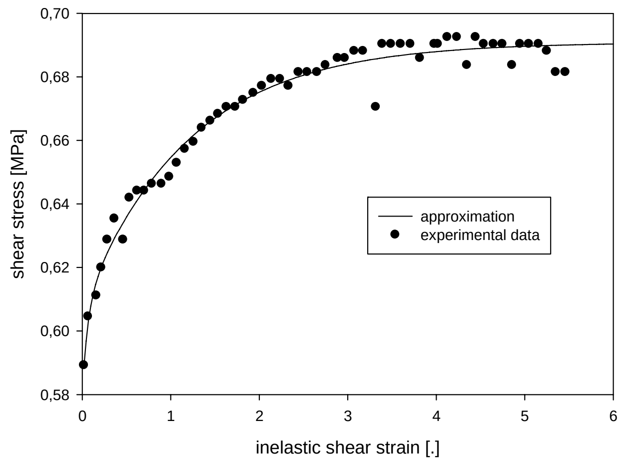


**Fig. 3.** Shear stress-inelastic shear strain plot, and a numerical approximation

$$\psi = \frac{\tau_0}{R_0}\left[m_1\left(R_1 - R_0\right) + m_2(R_0 + D_1)\right] - m_2\tau. \tag{11}$$

The expression (11) shows that, for small inelastic shear strains, the graph $\psi(\tau)$ must be linear with a slope $m_2$.

For the larger shear strains, the kinematic hardening is rapidly saturated, so $D \approx D_1$. Equations (3), (6), (10) then give:

$$\psi = \frac{\tau_0}{R_0} m_1 (R_1 + D_1) - m_1 \tau \ . \qquad (12)$$

The formula (12) indicates that for higher shear strains, the function $\psi(\tau)$ becomes linear again with a slope $m_1$.

To determine parameters $m_1$ and $m_2$, it is sufficient to calculate two slopes on both extremities of the curve $\psi(\tau)$ (Fig. 5) and according to (11), (12) the values of $\psi_s$ and $\tau_s$ can be found:

$$\psi_s = \frac{\tau_0}{R_0} \left[ m_1 \left( R_1 - R_0 \right) + m_2 (R_0 + D_1) \right], \tau_s = \frac{\tau_0}{R_0} \left( R_1 - D_1 \right) \qquad (13)$$

Equations (13) permit parameters $D_1$ and $R_1$ to be obtained. In the next part of this work we present the numerical solutions for obtained parameters.

## 4. NUMERICAL SOLUTION

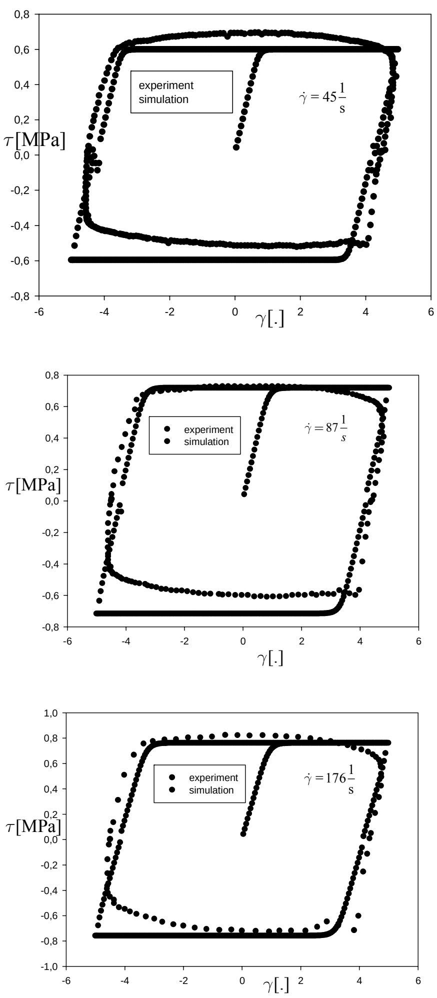


**Fig. 4.** Comparison of the experimental data and obtained results from numerical solutions by the Bodner-Partom law, for three different shear strain rates: $\dot{\gamma} = 45\frac{1}{s}, \dot{\gamma} = 87\frac{1}{s}, \dot{\gamma} = 176\frac{1}{s}$

Relations of shear strain-shear stress for three different shear rates (Fig.1) served for the identification of the Bodner-Partom model. Received parameters were used to numerical simulation. The calculation was made in the Excel program. The Euler's method was used to solve the equation (3). Numerically obtained results are compared with the experimental data for three different values
of the shear strain rate. We observe a good concordance between the experimental data with the numerical solution of Bodner-Partom model (Fig. 4).

## 5. CONCLUSIONS

In this paper, the constutive equations of the Bodner-Partom model are used for magnetorheological fluid in the damper. Conducted experiments on the Lord RD 1005-3 damper served for the identification of parameters of the B-P law. Experiments and the numerical results for three different values of shear strain rate validate the B-P model. The numerical model shows a good level of accuracy between the experimental and calculated data. It shows that the Bodner-Partom law, first allocated for metals, permits to describe the behaviour of magneto-rheological fluid in the damper.

More research is being conducted in order to improve the model behaviour, especially to accommodate the values of current in a coil.

### REFERENCES

1. **Bajkowski J.** (2005), Stanowisko badawczo dydaktyczne do wyznaczania wybranych charakterystyk tłumika lub amortyzatora magnetoreologicznego, *XXII Sympozjon PKM*, Gdynia-Jurata.
2. **Boder S. R., Partom I., Partom Y.** (1979), Uniaxial Cyclic Loading of Elastic-Viscoplastic Materials, *Journal of Applied Mechanics*, Vol. 46.
3. **Carlson J. D., Jolly M. R.,** (2000), MR fluid, foam and elastomer devices, *Mechatronics*, 10, 555-569.
4. **Chan K. S., Bodner S. R., Lindholm U. S**. (1998), Phenomenological Modeling of Hardening and Thermal Recovery in Metals, *Journal of Engineering Materials and Technology*, Vol. 110.
5. **Jimenez R., Alvarez-Icaza L**. (2005), *LuGre friction model for a magnetorheological damper*, Structural Control and Health Monitoring, Mexico.
6. **Spencer B. F., Dyke S. J., Sain M. K., Carslon J. D.** (1996), Phenomenological Model of a Magnetorheological Damper, *ASCE Journal of Engineering Mechanics*.
7. **Woźnica K., Pennetier O., Renard J.** (2001), Experiments and Numerical Simulations on Thin Metallic Plates Subjected to an Explosion, J*ournal of Engineering Materials and Technology*, Vol.123, 203-209.